

EVALUATION OF SELF-REPAIRING FLIGHT CONTROL SYSTEM BY WIND-TUNNEL FREE-FLIGHT DYNAMIC TEST

MATSUMOTO Yuji*, KAMEYAMA Takeharu*, SATAKA Masahiko**

* Third Research Center, Technical Research and Development Institute, Japan Defense Agency

** Mitsubishi Heavy Industries, Ltd., Nagoya Aerospace Systems

Keywords: *reconfigurable flight control, robust control, wind-tunnel free-flight test, flying qualities*

Abstract

Technical Research and Development Institute of Japan Defense Agency has been studying Self-Repairing Flight Control System [SRFCS], which is expected to improve flight safety and mission survivability by maintaining the same flying qualities in a damaged condition as those in the normal condition. Wind-tunnel free-flight dynamic tests were conducted to verify the performance of the prototype of this flight control system under the real aerodynamic condition. The H -infinity loop shaping design procedure and the pseudo command system concept were applied to this flight control system to have robustness and reconfigurability. The flyable wind tunnel model has twelve control surfaces including thrust-vectoring vanes, pneumatic thrust generator, inertial and air data sensors. Each control surface actuator has capability to simulate the failed or damaged conditions. High-pressured air tube, electronic power and data transfer cables are connected on the dorsal side of the model nearby the center of gravity. The model support system has three configurations: 3-Degree-of-Freedom [DOF], 4-DOF and 6-DOF. The 3-DOF configuration allows the model to rotate in three axes, and flying qualities researches were conducted with this configuration because of the dynamics similarities to free-flight in the air and its large rotation availability. The 4-DOF configuration allows the model to slide vertically along the strut. The 6-DOF means free-flight in the wind tunnel. Modified MIL-F-8785C flying qualities criteria were used to evaluate the dynamic free-flight tests results, which showed that the robustness and

reconfigurability of this flight control system were extremely effective in almost all of the simulated actuator failed and control surface damaged conditions.

1 Introduction

Enhancement of flight safety and mission effectiveness is not only the perpetual pursuit of aircraft designers but also the desire of users. In particular, the reconfigurable flight control system, which is expected to increase tolerance to the battle damage and/or control system failures, is the state-of-the-art. Technical Research and Development Institute [TRDI] of Japan Defense Agency has been studying Self-Repairing Flight Control System [SRFCS], which is expected to improve flight safety and mission survivability by its robustness and reconfigurability against the aerodynamic uncertainty and aircraft control system failures. A computer-based study of the SRFCS concept had been conducted [1] [2], and the robustness of the flight control system was verified. In succession to the computer-based study, the real-time hardware-in-the-loop simulation [HILS] was desired to verify the performance of the robustness and reconfigurability of the SRFCS under the real aerodynamic condition. TRDI decided to conduct the wind-tunnel free-flight dynamic tests. The flight control system and the wind-tunnel free-flight test technologies – including a flyable wind-tunnel model [WTM] – were developed simultaneously.

This paper presents an overview of the development of the flight control system based on the SRFCS concept and results of the wind-

tunnel free-flight tests.

2 Flyable Wind Tunnel Model Description

2.1. Flyable Wind Tunnel Model

The flyable WTM, shown in Fig. 1, has twelve control surfaces: a pair of canards, outboard flaps [OBF], inboard flaps [IBF], body flaps [BDF], rudders, and lateral-longitudinal thrust-vectoring vanes. The sensors in the WTM are inertial sensor and a boom-mounted air data sensor [ADS]. The unique designed ADS has high-AOA regime (about 30°) sensing availability [3]. Pneumatic thrust generator [PTG] is equipped in the model to balance out the model drag, and high-pressured air tube [HiPAT] is connected on the dorsal side of the model nearby its center of gravity. Electronic power supply and data transfer cables – they are called umbilical cables [UBC] in this study – are also connected there.

The flyable WTM is the dynamic scale model in order to represent the conceptual full-scale aircraft. Reference [4] gives scaling relations between the full-scale aircraft and the dynamic scale model: time is scaled to equal Froude number, and so on. Table 1 summarizes the factors needed to determine the dynamic scale model properties. σ_r is the ratio of air density at the altitude where the conceptual full-scale aircraft should fly to that of wind tunnel. The wind-tunnel free-flight dynamic tests are expected to simulate flight conditions: altitudes of 15,000-20,000 ft (4,572-6,096 m) and Mach 0.45. Scale ratio N_s is defined as about 8.7%, then the model wing span is about 1.0 m and length is about 1.4 m. Scale method constrains gross mass of the model around 17 kg [1]; dynamic response is about 3.4 times faster than that of the conceptual full-scale aircraft.

The model had to contain all of the equipments. Moreover, it had to have the efficient stiffness, which avoids structural coupling instability. Hence, the mainframe of the model was made from aluminum alloy, and body skin was from glass fiber reinforced plastic.

2.2. Dynamic Free-Flight Test Configurations

Dynamic wind-tunnel tests were conducted with three testing configurations: 3-DOF, 4-DOF and 6-DOF. Fig. 2 shows differences among these testing configurations.

The 3-DOF configuration allows the flyable WTM to rotate aligning three body axes but restrains translation motion. The 4-DOF configuration allows the flyable WTM to slide vertically in addition to three axes rotation. In the 6-DOF configuration, the flyable WTM is held by aerodynamic lift and pneumatic thrust in the test section. UBC, HiPAT and arresting wires are connected to the model during the test for each configuration. In addition, the design object configuration of the flight control system is the 6-DOF configuration.

3. SRFCS Design

3.1. SRFCS Design Outline

The SRFCS is a concept of flight control system to maintain the same flying qualities as that in the normal condition, even if the aircraft suffers from control disabilities. In this study, three technical features were considered for the SRFCS:

1. Robust Control
2. Fault Detection, Identification and Isolation [FDI] Technology
3. Control Commands Allocation

The robust controller must be designed to suit for the reconfiguration function. Design method of the robust controller – Inner-Loop Robust Controller [ILRC] – was H-infinity loop shaping design procedure [LSDP]. This design method enables designers to apply the classical controller design technique in specifying the main loop shape. The ILRC generates three moment-commands aligning with stability axes, which are called pseudo commands. The pseudo commands are input into the control commands allocation block [CAB] where these commands are converted to the optimal set of the actuator commands. Failure information is also input into the CAB. The linear control theory is applied to the ILRC and CAB design, and then non-linear effects – gravity and inertial coupling

– are compensated by the outer-loop compensator [OLC]. Fig. 3 shows the concept of the Research-SRFCS. Downsized dynamic scale model tends to move rapidly; hence, attitude and position hold autopilot [A&PH AP] controllers are required to conduct the wind-tunnel free-flight dynamic test. In addition, the Research-SRFCS has two gain sets: gain set for the low-AOA (about 8°) flight and for the high-AOA (about 30°) flight. They are derived from the bases of the Research-SRFCS designing outline showing on Table 2.

3.2. Control Allocation Method

The linearized mathematical models of the flyable WTM –the longitudinal and the lateral-directional mathematical models– were derived from aerodynamic data by the static wind tunnel tests. Disturbances induced by the UBC and the HiPAT were expected to interfere the motion of the flyable WTM. Such effects were treated as uncertainties in designing the flight controller. Additionally, the nominal control model of the flyable WTM must be designed to adapt to the pseudo commands.

The nominal control model and the state equation of the flyable WTM is described as

$$G = \{A, B, C, D\} \quad (1)$$

$$\dot{x} = Ax + B^* \delta^*, \quad (2)$$

where δ^* is a vector of generalized controller outputs. The matrix B^* is derived from

$$B^* \delta^* = B \delta, \quad (3)$$

where δ , an actuator deflection vector, is described as follows:

$$\delta = B^\# B^* \delta^* \quad (4)$$

$B^\#$ in equation (4) is a generalized inverse matrix of B .

Since the elements of the vector δ are actuator deflection commands input into each actuator, δ has larger number of element than δ^* has. Consequently, a set of the elements in δ cannot be determined from the equation (4) uniquely. To decide the actuator deflection vector δ , a designer may select the pseudo inverse matrix

that minimizes the norm of δ among generalized inverse matrices of B . In addition, the diagonal weighted matrix and the pseudo inverse matrix shown in the equation (5) are applied to authorize each deflection angle appropriately:

$$\begin{aligned} \delta &= B^\dagger B^* \delta^* = (NN^\dagger) B^\dagger B^* \delta^* \\ &= N(BN)^\dagger B^* \delta^* = T \delta^*, \end{aligned} \quad (5)$$

where N is a diagonal weighted matrix and the matrix with a symbol “ \dagger ” means a pseudo-inverted matrix. The matrix T allocates the pseudo-commands to each control surface actuator as deflecting command, therefore T is called the commands allocating matrix. A designer can apply a unit matrix to B^* without losing generality.

The flight control system designed by the pseudo-command method always outputs moment commands even in the degraded control condition, while the conventional flight control system is required to coordinate the feedback gains in order to generate appropriate commands. In addition, the weighted diagonal matrix allows not only arbitrary allocation of the actuator deflection commands but also isolation of the signals coming from and feeding to the damaged control devices. When the failure signals are input into the CAB, the commands allocating matrix T is tailored in accordance with the procedure mentioned above.

3.3. Inner Loop Robust Controller [5]

The nominal model for the ILRC is derived from the 6-DOF configuration of the flyable WTM. Differences from the other configurations are treated as the model uncertainties. This section describes the longitudinal ILRC for low-AOA regime as an example of the ILRC design process.

The longitudinal nominal model is described as $G = \{A, B, C, D\}$. The short-period mode model is applied in order to reduce the order of the controller, then this is represented by $G_{sp} = \{A_{sp}, B_{sp}, C_{sp}, D_{sp}\}$. The state equation of the short-period mode is

$$\dot{x}_{sp} = A_{sp} x_{sp} + B_{sp}^* \delta^* \quad (6)$$

$$\delta = T \delta^* = N(B_{sp} N)^{\dagger} B_{sp}^* \delta^*, \quad (7)$$

where the state vector is $x_{sp}^T = [\alpha \ q]$, and the matrix B_{sp}^* equals to unit matrix. The control command δ^* is the pitch rate command, and the output vector is $y^T = [\alpha \ q]$. Then, the plant applied the pseudo-command method is described as $G_{sp}^* = \{A_{sp}, B_{sp}^*, C_{sp}, D_{sp}\}$. Consequently, the longitudinal ILRC is designed for the plant G_{sp}^* of which feedback signals consist of the pitch rate and the AOA. The design procedure is as follows:

STEP 1: The state variables are AOA and pitch rate; scaling operation is not required.

STEP 2: The controller $K(s)$ is designed using LSDP. The plant G_{sp}^* is shaped by the pre- and post-compensators $W_1(s)$ and $W_2(s)$, which are described as follows:

$$W_1(s) = K_{qc} \quad (8)$$

$$W_2(s) = \begin{bmatrix} K_{\alpha} & 0 \\ 0 & \frac{(K_1 s + K_2)(K_3 s + 1)(K_5 s + 1)}{s(K_4 s + 1)(K_6 s + 1)} \end{bmatrix} \quad (9)$$

Required controlling-band and roll-off-rate are decided using singular-value-plots of G_{sp}^* and the shaped plant “ $W_2(s) G_{sp}^* W_1(s)$ ”. These singular-value-plots are shown in Fig. 4.

STEP 3: The controller $K(s)$ is obtained from “ $W_2(s) G_{sp}^* W_1(s)$ ” using the normalized coprime factorization approach. This design algorithm is shown in the reference [5]. The stability margin ε of the shaped plant is acceptable value of 0.506 ($\gamma = 1.98$). Moreover, the gap metrics between G_{sp}^* and “ $W_2(s) G_{sp}^* W_1(s)$ ” are obtained as Fig. 5, and the maximum gap distance is derived as 0.25.

Thus, these results give a perspective that the controller can stabilize the flyable WTM not only with the 6-DOF configuration but also with the 3- and 4-DOF configurations. The singular-value-plots of required open loop and after-shaping open loop transfer functions are shown in Fig. 6. From this figure, it is shown that the singular values of the after-shaping open loop transfer function are achieved nearby those of the required open loop.

3.4. Attitude and Position Hold Autopilot

The A&PH AP controller applied Proportional-Integral-Derivative [PID] method is unique for the free-flight tests in order to stable the flyable WTM in the wind-tunnel test section. The diagram of the autopilot controller is shown in Fig. 7. In the front-side regime, downrange position is controlled with thrust changing controlled by valve divergence of the thrust generator, while cross-range position and altitude are controlled with bank and pitch-up through the AH-AP respectively. In the backside regime, altitude is controlled by Direct Lift Control [DLC] method using direct control surface deflection, while downrange position is controlled by drag change produced by AOA change. Cross-range position control is the same as that in the front-side regime.

4 Dynamic Free-Flight Testing System

This study was conducted in the low speed wind tunnel of the 3rd Research Center of TRDI. This wind tunnel is an open-type circulating tunnel, and the test section dimension is about 3- by 3-meter. The Dynamic Free-Flight Testing System [DFFTS] consists of six apparatuses:

1. Research-SRFCS Computer
2. Hardware Control Computer
3. Flyable WTM Support System
4. Safety Devices
5. Optical Position Measurement System
6. High-Pressured Air Supply System

Fig. 8 shows an overview of the DFFTS.

The Research-SRFCS software is installed in the Research-SRFCS computer. The Research-SRFCS computer receives sensor data through the Hardware Control Computer [HCC], generates deflection angle commands and feeds the commands to the HCC in real-time, while the HCC receives deflection angle commands and converts them to actuation commands. In addition, the HCC can generate simulated control disabilities, process sensor signals, acquire flight data, and execute flight preparation test.

The flyable WTM Support System has three support struts: one main strut and two sub-struts.

The main strut is connected to the ventral side of the flyable WTM through the support system interface, which allows three axes rotation by gimbals mechanics. If a top section of the main strut is exchanged to the slide-allowable part, vertical motion is available. The sub-struts support the model at the fore and aft body until the model has trimmed in the airflow. Each strut has a touch sensor to detect the trim condition. In free-flight testing, all the struts are pulled down and the test section is cleared.

Safety devices capture the flyable WTM when dynamic wind-tunnel test is finished or the model is to be under dangerous condition. The safety device consists of following parts:

1. Flyable WTM Arresting Wires
2. Capturing Net
3. Protective Net Screen

The Optical Position Measurement System [OPMS] measures position of the model. The position data are used for the PH-AP controller.

The high-pressured air supply system consists of an air compressor, a cooling device, an air storage tank, and a supplying pipe. The commercially available air compressor creates high-pressured air of which discharge pressure is about 13 kgf/cm^2 (1,275 kPa). High-pressured air is supplied from the air storage tank to the PTG through the supplying pipe.

5 Evaluation Concept

5.1. Evaluation Items

The evaluation items are listed below:

1. Robustness of the Research-SRFCS
 - off-design configurations (3- and 4-DOF)
 - high-AOA aerodynamic conditions
 - off-design flight conditions (AOA $8^\circ \sim 30^\circ$)
 - control disabilities
2. Reconfigurability of the Research-SRFCS
 - control disabilities
3. Free-flight in the wind tunnel

5.2. Flying Qualities Criteria Modification

This study uses the criteria for evaluation of flying qualities, such as short-period, Dutch-roll and roll-mode of a Class IV aircraft in flight phase category A specified in reference [6].

However, the flying qualities requirements cannot be applied directly because of following issues:

- a) High responsive scaled model
- b) Safeness of the tests
- c) Application of only one control law

Longitudinal maneuvering characteristics in short-period are specified by the frequency requirements swept with Nz/α and the damping ratios. Considered by issue a), the frequency requirements should be multiplied by $1/\sqrt{Ns} \approx 3.4$, while the damping ratios should be applied directly because of non-dimensional. However, issue c) restricts such high response because high gains used in high responsive controller may have malign influences upon other test configurations. Therefore, stabilizing the flyable WTM inside the test section and satisfying the issue b) will be adequate requirement for the test. Consequently, upper bound of the short-period frequency requirement: $\omega_{nsp}^2/(Nz/\alpha) = 3.6$ is modified by multiplying scaled response value $1/\sqrt{Ns} \approx 3.4$, i.e. $\omega_{nsp}^2/(Nz/\alpha) = 41.38$, while lower bound of that is not modified. Fig. 9 shows the short-period frequency requirements for this study.

Similarly, lower bound of the Dutch-roll frequencies requirements are applied the values specified in [6], and damping ratio requirements are also not modified.

Level 1 upper boundary of roll-mode time constants is specified by [6] as 1.0 second, and the value is applied here.

5.3. Motion Excitation Command

Flying qualities are acquired from time histories of the pitch and Dutch-roll oscillations and the roll maneuver, therefore an adequate motion of the flyable WTM must be excited to acquire each flying quality. The motion excitation commands are defined as shown in Table 3. When each command is input into the flyable WTM, the A&PH AP are disengaged.

5.4. Simulated Control Disabilities

The simulated control disabilities are categorized as following three aspects:

1. Actuator Failure [FAIL]
2. Actuator Hard Over [HO]

3. Control Surface Damage [DMG]

The simulated FAIL is realized by reducing the actuation gains to intended percentage. Therefore, the deflection angle decreases by the FAIL in accordance with the gain reduction percentage. The simulated HO is realized by freezing the intended actuator in the maximum deflection angle, and represents an aerodynamic anomaly. The simulated DMG generates aerodynamic moment that will be occurred if the intended surface area is damaged and dropped out. The damage scale is expressed as percentage. Aerodynamic moment is simulated by each control surface deflection. As there are several combinations of simulated control disabilities, this paper presents the results of the single HO and multiple DMG cases.

5.5. FDI and Reconfiguration Time Lag

Failure detection and isolation technology was subsequent issue of this study; therefore, failure was treated as given information. This study used FDI time lag defined as follows.

X + 0.0 sec.	Failure(s) Occurring
X + 0.5 sec.	FDI Start
X + 0.7 sec.	FDI Complete

5.6. Test Configurations and Evaluation

Dynamics analyses – representative result is shown in Fig. 10 – illustrate that dynamic characteristics of the model supported by the 3-DOF configuration are similar to the ones in free-flying without UBC and HiPAT. Therefore, the 3-DOF configuration is selected to evaluate the flying qualities. The 4-DOF configuration is used to determine the trim condition and evaluate robustness against off-design conditions. The free-flight (6-DOF) tests would not appropriate to flying qualities research because of A&PH-AP engagements. Therefore, a series of the 6-DOF tests were regarded as a qualitative study for the design method of a reconfigurable flight control system.

6 Test Process

In this study, a series of the tests with the 3- and 4-DOF configurations were also regarded as steps toward the free-flight (6-DOF) test. The

free-flight (6-DOF configuration) tests were conducted by following process:

- (1) Mounting the flyable WTM in 4-DOF conf. without the main strut top stopper
- (2) Setting the initial AOA lower than intended flight condition for avoiding accidental lift-off, and increasing wind speed
- (3) After trimming, descending the main strut quite a few distance and engaging PH-AP
- (4) Lifting up the model to initial position
- (5) Checking the forces exerted on the model
- (6) Trimming, then getting down the strut steeply
- (7) Making free-flight

7 Results and Discussions ^[7]

Flying qualities at low- and high-AOA condition were surveyed for the 3-DOF configuration. Fig. 11 shows time histories of the low-AOA OBF HO injected case on the 3-DOF configuration. The responses with reconfiguration, in particular beta response, gave steeper regulation than the ones without. Fig. 12 shows time histories of all the one-side control surfaces simulated 100% damage case at low-AOA regime. This condition simulated aerodynamic moments as all the area of four control surfaces – IBF and OBF, BDF and rudder – were removed. In particular, the responses by beta doublet obviously show the difference of the convergence between reconfigured case and non-reconfigured one. Acquired data of flying qualities are summarized in Fig. 15, which shows that not only well-conditioned but also control disabled cases are satisfied Level 1 requirement of short-period and Dutch-roll mode. Moreover, the 3-DOF is the off-design configuration for the Research-SRFCS; the ILRC has satisfying robustness against difference among the configurations.

Simulated 100 % OBF DMG injected case results on the 6-DOF are shown in Fig. 13. Large transition was occurred when the simulate DMG was injected; nevertheless the position and the attitude of the flyable WTM were stabilized during about 30 seconds after the

EVALUATION OF SELF-REPAIRING FLIGHT CONTROL SYSTEM BY WIND-TUNNEL FREE-FLIGHT DYNAMIC TEST

injection of the commands. Fig. 14 shows time histories of the responses excited by the commands specified in Table 4, and the derived flying qualities data are plotted in Fig. 15. Dutch-roll characteristics of the high-AOA 6-DOF are out of Level 1 region, however, the time histories show the motion of the WTM stabilized.

8. Conclusions

This paper presents the designing results of the reconfigurable flight control system for the Self-Repairing Flight Control System and wind-tunnel free-flight test results. The H-infinity loop shaping design procedure was used for its inner loop robust controller. Reconfigurability of the flight controller is realized by the pseudo-command method. Its robustness and reconfigurability were evaluated by wind-tunnel free-flight dynamic tests, and verified that this flight control system possesses intended ability as follows:

1. Robustness against off-design configuration at low- and high-AOA regimes
2. Robustness against aerodynamic uncertainty at high-AOA regime
3. Robustness against off-design flight conditions
4. Robustness and reconfigurability for control disabilities
5. Free-flight at low- and high-AOA regime

TRDI is also studying the FDI technology, and planning a project to verify total SRFCS.

References

- [1] KAMEYAMA Takeharu, et al. The Study on Self Repairing Flight Control System – Overview of Self Repairing Flight Control Law, *The 36th Aircraft Symposium*, (in Japanese), The Japan Society for Aeronautical and Space Sciences, Oct. 12-14, 3A1, pp.457-460, 1998.
- [2] KAMEYAMA Takeharu, et al. The Study on Self Repairing Flight Control System – Inner Loop Robust Control Law Design, *The 36th Aircraft Symposium*, (in Japanese), The Japan Society for Aeronautical and Space Sciences, Oct. 12-14, 3A2 pp.461-464, 1998.
- [3] ISHIGURO Mitsuo, et al. The Study on Self Repairing Flight Control System – The Design of The Dynamic Free-Flight Wind Tunnel Test System, *The 39th Aircraft Symposium*, (in Japanese), The Japan Society for Aeronautical and Space Sciences, Oct. 29-31, 2B6, pp.322-327, 2001.
- [4] Scherberg, M. and Rhode, R.V. *Mass Distribution and Performance of Free Flight Models*, NACA TN 268, 1927.
- [5] MASUKO Yoichiro, et al. The Study on Self Repairing Flight Control System – The Design of Self Repairing Flight Control System, *The 39th Aircraft Symposium*, (in Japanese), The Japan Society for Aeronautical and Space Sciences, Oct. 29-31, 2B6, pp.315-321, 2001.
- [6] Military Specification. *Flying Qualities of Piloted Airplanes*, MIL-F-8785C, 1980.
- [7] MATSUMOTO Yuji, et al. The Study on Self Repairing Flight Control System –The Results of the Dynamic Free-Flight Wind-Tunnel Testing, *The 39th Aircraft Symposium*, (in Japanese), The Japan Society for Aeronautical and Space Sciences, Oct. 29-31, 2B6, pp.328-337, 2001.

Table 1 Scale Factors

Quantities	Scale Factors
Linear Dimension	Ns
Relative Density [$m/\rho l^3$]	1
Froude Number [V^2/lg]	1
Time	\sqrt{Ns}
Angular Velocity	$1/\sqrt{Ns}$
Linear Acceleration	1
Linear Velocity	\sqrt{Ns}
Weight	Ns^3/σ_r

Table 2 Research-SRFCS Designing Outline

Low AOA Gain Set		High AOA Gain Set	
Alt. 0m, AOA 8°, Flow rate 42m/s		Alt. 0m, AOA 30°, Flow rate 20m/s	
Three angular-acceleration pseudo commands			
Control Allocation: Pseudo-Inverse matrix with weightings			
Reconfiguration: setting the weighting(s) of damaged control surface(s) to zero, allocating control commands to the rest control surfaces			
ILRC: H-infinity LSDP			
Longitudinal	Command: Pitch Rate Feedback: AOA, Pitch Rate Two degree of freedom control by inverse dynamics		
Lateral / Directional	Command: Stability Axis Roll Rate, Sideslip Angle Feedback: Stability Axis Roll Rate, Stability Axis Yaw Rate, Sideslip Angle		
A&PH Autopilot Controller (PID)			
AH	Pitch Hold: Pitch Rate Command Bank Hold: Stability Axis Roll Rate Command		
Cross Range PH: Bank Angle Command			
PH	Altitude Hold:	Altitude Hold:	
	Pitch Angle Command	DLC command	
PH	Downrange Hold:	Downrange Hold:	
	Thrust Control Command	Pitch Angle Command	

Table 3 Motion Excitation Commands

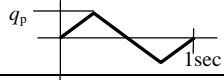
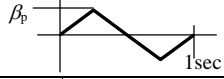
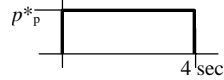
Motion Excitation Commands		
Short-Period	Pitch rate q_p : 10°/sec 1Hz Doublet	
Dutch-Roll	Sideslip angle β_p : 2° 1Hz Doublet	
Roll-Mode	Stability axis roll rate p^*_p : 5°/sec 4sec Step	

Table 4 Motion Excitation Commands for 6-DOF

Mode	Excitation Commands	
	Low-AOA	High-AOA
Short Period	q_p : 8°/sec 1 Hz Doublet (PH-AP on)	q_p : 10°/sec 1 Hz Doublet (PH-AP on / off)
Dutch-Roll	β_p : 2° 1 Hz Doublet (PH-AP on)	β_p : 2° 1 Hz Doublet (PH-AP on / off)
Roll-Mode	p^*_p : 10°/sec 0.5 Hz Doublet (PH-AP on)	p^*_p : 20°/sec 1 Hz Doublet (PH-AP on)

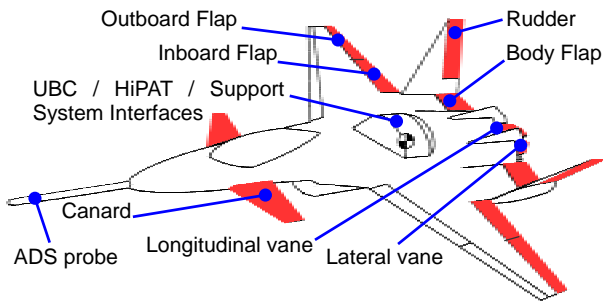


Fig. 1 Flyable WTM

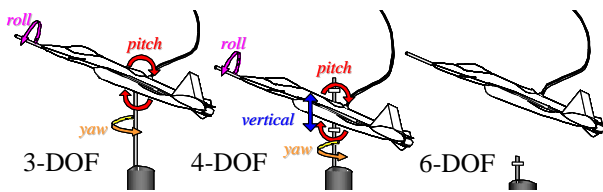


Fig. 2 Testing Configurations

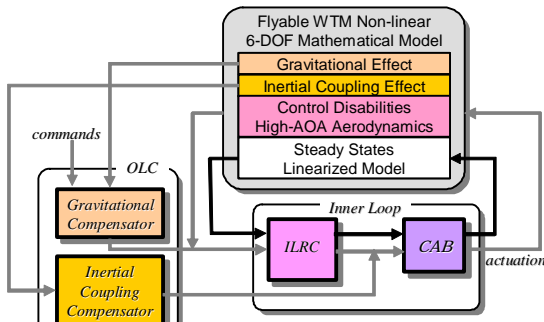


Fig. 3 Concept of the Research-SRFCs

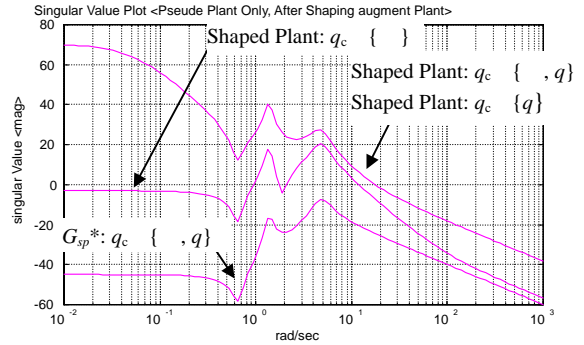


Fig. 4 Singular-Value-Plots of G_{sp}^* and Shaped Plants

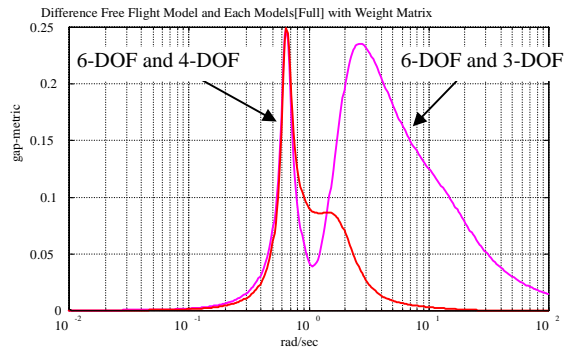


Fig. 5 Gap Metrics between G_{sp}^* and “ $W_2(s) G_{sp}^* W_1(s)$ ”

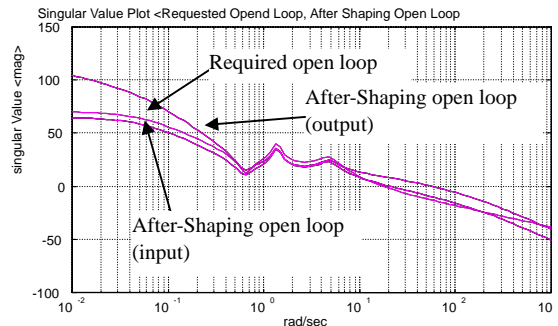


Fig. 6 Singular-Value-Plots of Required Open Loop and After-Shaping Open Loop

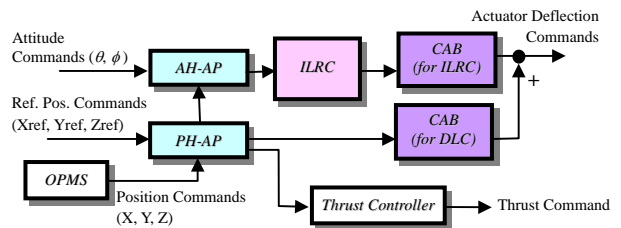


Fig. 7 Attitude and Position Holding Autopilot Diagram

EVALUATION OF SELF-REPAIRING FLIGHT CONTROL SYSTEM BY DYNAMIC FREE-FLIGHT WIND-TUNNEL TEST

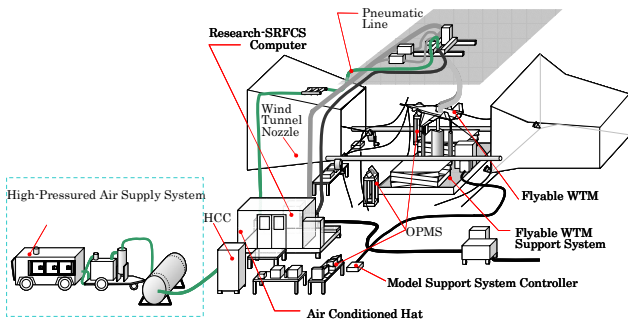


Fig. 8 Overview of DFSTS

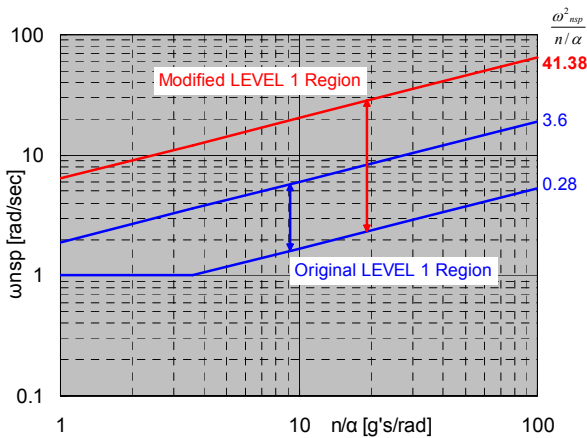


Fig. 9 Modification of Short-Period Frequency Requirements (Category A) [6]

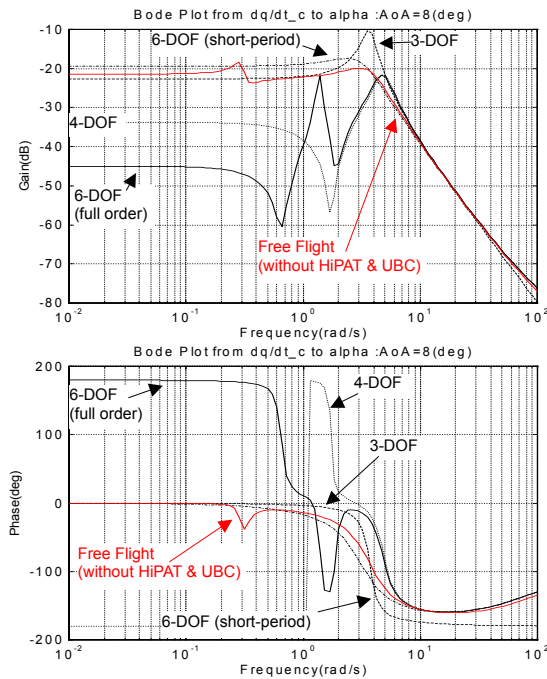


Fig. 10 Dynamic Analyses of Testing Configurations
Solid: 6-DOF full order model / Dashed: 6-DOF short-period / Dotted: 4-DOF / Chained: 3-DOF / Red-Solid: Free Flight without HiPAT & UBC

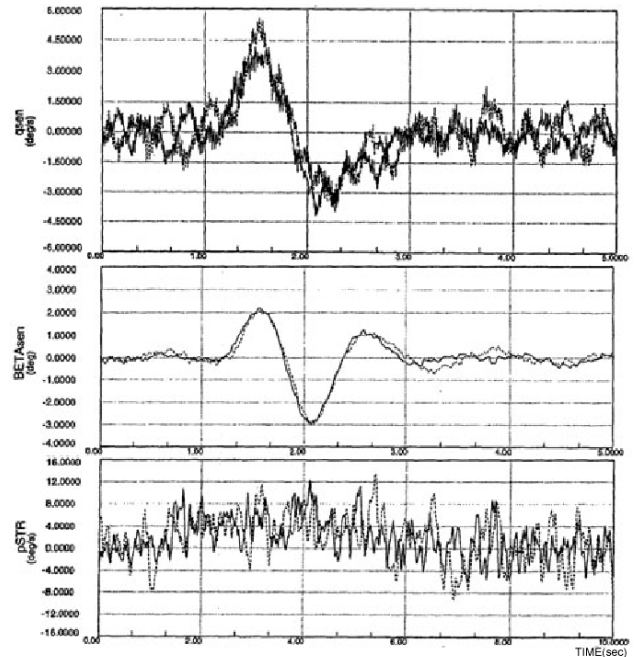


Fig. 11 Responses of 3-DOF Configuration in Low-AOA with OBF HO by Motion Excitations
Solid: reconfigured / Dotted: non-reconfigured

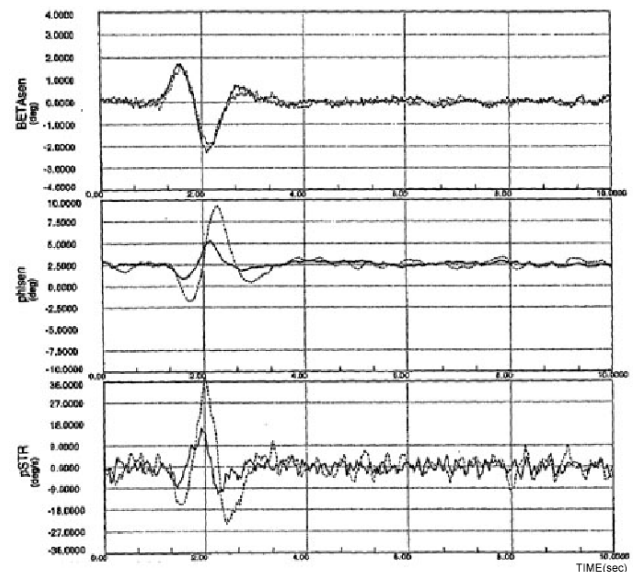
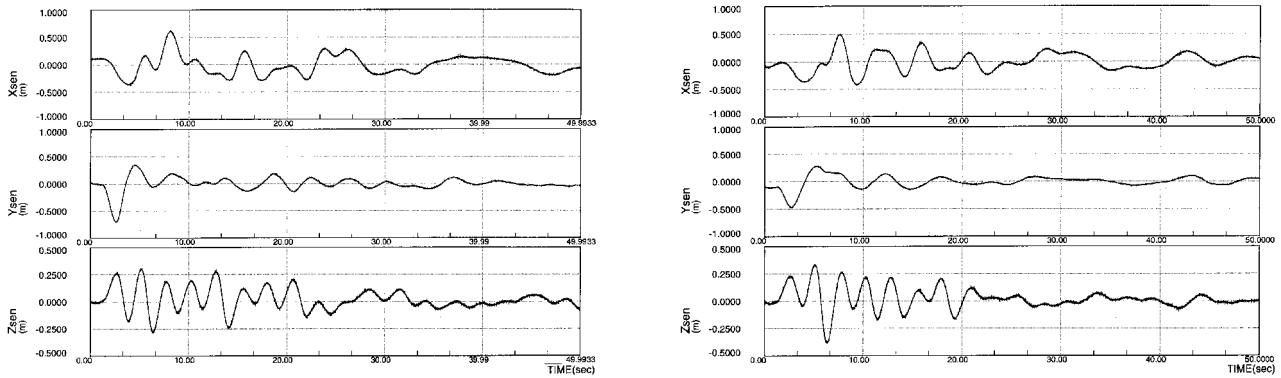
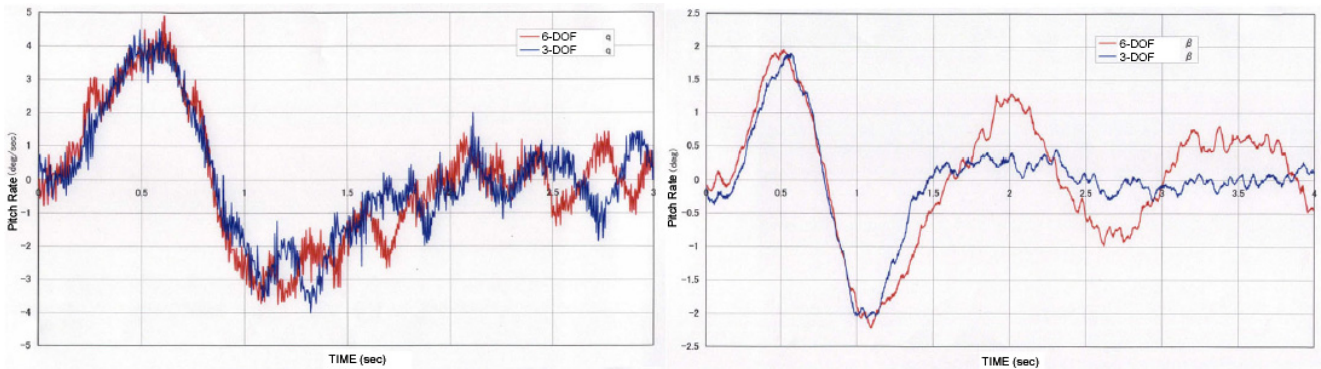


Fig. 12 Responses of 3-DOF Configuration in Low-AOA with One-Side Surfaces 100% DMG by Beta Doublet
Solid: reconfigured / Dotted: non-reconfigured



(a) Non-Reconfigured (b) Reconfigured
 Fig. 13 Responses of 6-DOF in Low-AOA with OBF 100% DMG



(a) Longitudinal Responses (b) Directional Responses
 Fig. 14 Responses of 6-DOF High-AOA PH-AP Disengaged and 3-DOF

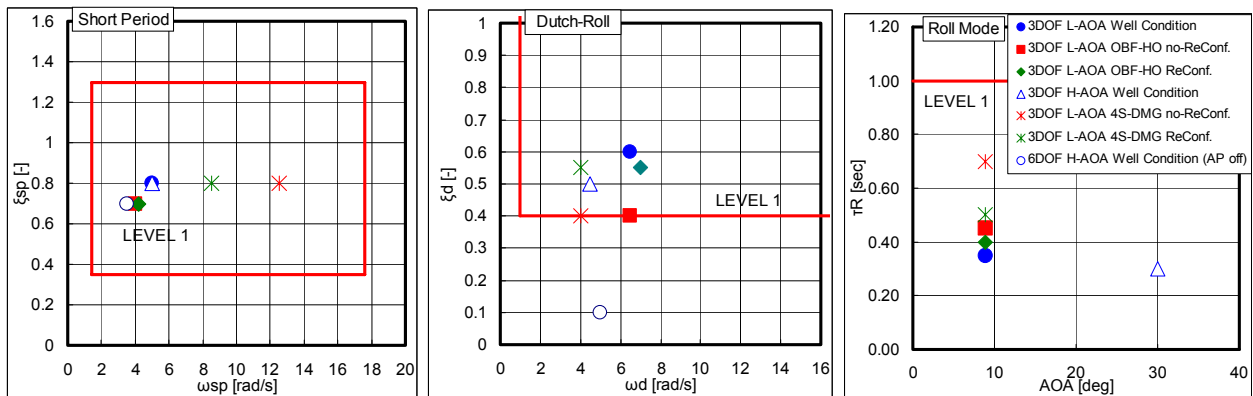


Fig. 15 Flying Qualities